

Inhibitive effect of new synthesized imidazopyridine derivatives for the mild steel corrosion in Hydrochloric acid medium

S. Bourichi¹, Y. Kandri Rodi^{1*}, M. EL Azzouzi^{3*}, Y. Kharbach²,
F. Ouazzani Chahdi¹, A. Aouniti³

¹Laboratory of Applied Organic Chemistry, U.S.M.B.A., Faculty of Science and Technology of Fes, Morocco.

²Laboratory of Applied Chemistry, U.S.M.B.A., Faculty of Science and Technology of Fes, Morocco.

³LC2AME, Faculty of Science, Mohammed Premier, University, Po Box 717, 60000 Oujda, Morocco.

Received 20 Jun 2016,
Revised 17 Oct 2016,
Accepted 23 Oct 2016

Keywords

- ✓ mild steels,
- ✓ imidazopyridine,
- ✓ Corrosion Inhibitors,
- ✓ Impedance,
- ✓ Adsorption,
- ✓ SEM.

M. EL Azzouzi
azzouzi16@hotmail.com
+212-675-414-044

Abstract

The effect of new synthesized imidazopyridine derivatives Pyr1 and Pyr2 on the corrosion inhibition of mild steel in 1 M HCl at the room temperature was studied by weight loss and different electrochemical techniques such as electrochemical impedance spectroscopy (EIS), potentiodynamic polarization. Weight-loss essays confirm that the corrosion rate decreases as the Pyr1 and Pyr2 concentration increases. The inhibition efficiency for those compounds studied increased with the increase of inhibitor concentrations to attain 91% for Pyr1 and 85% for Pyr2 at 10^{-3} M. The potentiodynamic polarization curves indicated that Pyr1 and Pyr2 acted as a mixed-type inhibitor in hydrochloric acid. Adsorption of Pyr1 and pyr2 on the mild steel surface in 1 M HCl follows the Langmuir isotherm model, and SEM characterization of the steel surface was made. The SEM micrographs show a smooth surface in the presence of Pyr1 and Pyr2 compared with absence of the inhibitors.

1. Introduction

Acids are increasingly used in industry, they are used such as acid cleaning, acid descaling, acid pickling and oil wells acidizing. Hydrochloric acid is one of the most used acids. Because of the aggressiveness of acid solutions, inhibitors are ordinarily used to reduce the corrosive attack of steel. Mild steel is widely used in chemical industries due to its low cost [1-5].

Among the inhibitors used there are organic inhibitors acting by adsorption, which is facilitated by nitrogen, oxygen, sulfur, double bonds and aromatic rings [6-18]. Many *N*-heterocyclic compounds such as derivatives of imidazole [19-22], pyridine [23-26], pyrimidine [27], pyridazine [28-30] and imidazopyridine [31] have been reported as effective corrosion inhibitors for steel in acidic media.

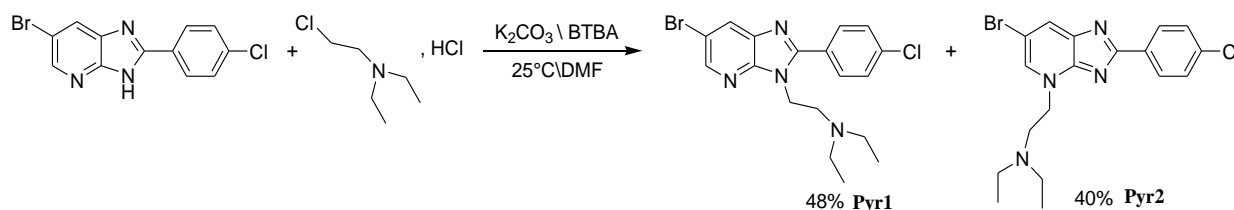
In the present paper, two regioisomers imidazopyridine derivatives newly synthesized “2-(6-bromo-2-(4-chlorophenyl)-3*H*-imidazo[4,5-*b*]pyridin-3-yl)-*N,N*-diethylethanamine” (Pyr1) and “2-(6-bromo-2-(4-chlorophenyl)-4*H*-imidazo[4,5-*b*]pyridin-4-yl)-*N,N*-diethylethanamine” (Pyr2) was tested as corrosion inhibitor for mild steel in 1M HCl. The corrosion inhibitive activity of those organic compounds was examined successively via weight loss, potentiodynamic polarization curves and electrochemical impedance spectroscopy (EIS). The kinetic and adsorption parameters of corrosion inhibition process are also evaluated. The scanning electron micrographs (SEM) of steel surface were taken in 1 M HCl with and without inhibitors.

2. Materials and methods

2.1. Experimental section

2-(6-bromo-2-(4-chlorophenyl)-3*H*-imidazo[4,5-*b*]pyridin-3-yl)-*N,N*-diethylethanamine and its regioisomer were synthesized according to the following procedure : The mixture of 0,2g (0,64mmol) of 6-bromo-2-(4-chlorophenyl)-3*H*-imidazo[4,5-*b*]pyridine dissolved in 25ml of DMF, and potassium carbonate K_2CO_3 0,12g (0,91mmol) is stirred magnetically hang for 5 minutes and then added 0.07g (0,22mmol) of tetra-*n*-

butylammonium (TBAB) and 1,2 equivalent of 2-Chloro-*N,N*-diethylethylamine hydrochloride. Stirring was continued at room temperature for 6 hours. After removing salts by filtration, the DMF is evaporated under reduced pressure and the residue obtained is dissolved in dichloromethane. The remaining salts are extracted with distilled water and the resulting mixture is chromatographed on silica gel column (eluent: ethyl acetate/Hexane (1/3)), giving both regioisomer Pyr1 and Pyr2 (Scheme 1) [32].



Scheme 1: Synthesis of the new compounds Pyr1 and Pyr2

Pyr 1: 2-(6-bromo-2-(4-chlorophenyl)-3H-imidazo [4, 5-b]pyridin-3-yl)-*N,N*-diethylethanamine

Yield 48%; F(°C) = 218-220; R_f : 0.87 ; ¹H NMR (CDCl₃; 300MHz): 8.48 (d, 1H, H_{py}, J=2.1Hz) ; 8.28 (d, 1H, H_{py}, J=2.1Hz) ; 7.69-7.54 (m, 2H, H_{Ar}) ; 7.50-7.48 (m, 2H, H_{Ar}) ; 4.42 (t, 2H, N_{imid}CH₂) ; 2.72-2.68 (m, 2H, CH₂) ; 2.38- 2.25 (m, 4H, CH₂) ; 0.88 (t, 6H, CH₃).

*RMN ¹³C (CDCl₃) δ ppm: 154.83, 147.43, 137.19, 129.92, 114.67(C_q); 145.31, 130.42, 129.92, 129.34, 114.62(CH_{Ar}); 50.84, 46.46, 41.43 (CH₂); 9.69 (CH₃).

Pyr 2: 2-(6-bromo-2-(4-chlorophenyl)-4H-imidazo[4,5-b]pyridin-4-yl)-*N,N*-diethylethanamine

Yield 40%; viscous; R_f : 0.57 ; ¹H NMR (CDCl₃; 300MHz): 8.45 (d, 1H, H_{py}, J=2.1Hz) ; 8.20 (d, 1H, H_{py}, J=2.1Hz) ; 7.92-7.86 (m, 2H, H_{Ar}) ; 7.61-7.49 (m, 2H, H_{Ar}) ; 4.45-4.44 (t, 2H, N_{imid}CH₂); 2.85-2.84 (t, 2H, CH₂) ; 2.45- 2.38 (m, 4H, CH₂) ; 0.80 (t, 6H, CH₃).

*RMN ¹³C (CDCl₃) δ ppm: 155.21, 147.50, 136.24, 129.84, 114.14(C_q); 145.3, 130.74, 129.10, 114.62(CH_{Ar}); 51.62, 47.46, 42.87(CH₂); 10.01(CH₃).

2.2. Materials preparation

We used mild steel with a chemical composition (in wt%) of 0.09%P, 0.01 % Al, 0.38 % Si, 0.05 % Mn, 0.21 % C, 0.05 % S and the remainder iron (Fe). Before using the samples have undergone polishing with emery paper Sic (220, 400, 800, 1000 and 1200), then they were washed with distilled water, degreased with acetone, washed again with bidistilled water, and dried at room temperature before use.

2.3. Solutions

The aggressive solutions of 1M HCl were prepared by dilution of analytical grade 37% HCl with distilled water. The concentration range of Pyr1 and Pyr2 was 10⁻⁶ M to 10⁻³ M.

2.4. Gravimetric measurements

Gravimetric measurements were performed according to the standard methods, the steel specimens used had a rectangular form 1.5 cm × 1.5 cm × 0.03 cm, after being polished and washed with distilled water and acetone, samples were accurately weighed and then immersed in 50 mL of a 1M HCl solution with and without addition of different concentrations of inhibitors. The immersion time was 6 h at room temperature. Then the specimens were taken out, washed, dried, and weighed accurately. In order to get good reproducibility, all measurements were performed few times and average values were reported.

2.5. Electrochemical measurements

The electrochemical measurements were carried out using Volta lab (Tacussel- Radiometer PGZ 100) potentiostat and controlled by Tacussel corrosion analysis software model (Voltmaster 4) at under static condition. The corrosion cell used had three electrodes. The reference electrode was a saturated calomel electrode (SCE). A platinum electrode was used as auxiliary electrode of surface area of 1 cm². The working

electrode was mild steel of the surface 0.04 cm^2 . All potentials given in this study were referred to this reference electrode. The working electrode was immersed in test solution for 30 min to establish steady state open circuit potential (E_{ocp}). After measuring the E_{ocp} , the electrochemical measurements were performed. All electrochemical tests have been performed in aerated solutions at 308 K.

The EIS experiments were conducted in the frequency range with high limit of 100 kHz and different low limit 0.1 Hz at open circuit potential, with 10 points per second, at the rest potential, after 30 min of acid immersion, by applying 10 mV ac voltage peak-to-peak. Nyquist plots were made from these experiments. The best semicircle can be fit through the data points in the Nyquist plot using a non-linear least square fit so as to give the intersections with the x -axis.

After AC impedance test, the potentiodynamic polarization measurements of mild steel substrate in inhibited and uninhibited solution were scanned from cathodic to the anodic direction, with a scan rate of 1 mV s^{-1} . The potentiodynamic data were analysed using the polarization VoltaMaster 4 software. The linear Tafel segments of anodic and cathodic curves were extrapolated to corrosion potential to obtain corrosion current densities (I_{corr}).

2.6. SEM study

Polished mild steel specimens were tested without inhibitor and with the concentration of inhibitors solutions in 1M hydrochloric acid. Then they were washed with distilled water, dried and analyzed by SEM (FEI Quanta 200). The acceleration voltage employed was 0.5 to 30 kV with a resolution of 3.5nm.

3. Results and discussion

3.1. Weight Loss Measurements

Using the weight loss data, we calculated the corrosion rates of mild steel and the efficiencies inhibition for various concentrations of products Pyr1 and Pyr2 at 308 K in 1M HCl solution. The results are reported in Table1. The inhibition efficiency ($\eta_{\text{WL}}\%$) and surface coverage (θ) were calculated as follows:

$$C_R = \frac{W_b - W_a}{At} \quad (1)$$

$$\eta_{\text{WL}}(\%) = \left(1 - \frac{w_i}{w_0}\right) \times 100 \quad (2)$$

$$\theta = \left(1 - \frac{w_i}{w_0}\right) \quad (3)$$

Where W_b and W_a are, respectively, the weights of the specimens before and after exposure to 1 M hydrochloric acid, w_0 and w_i are the values of corrosion weight losses of mild steel in uninhibited and inhibited solutions, respectively; A is the total surface area of the mild steel specimen (cm^2) in this investigation and t is the time of exposure (h). According to the results in Table 1 the corrosion rate decreases with increasing concentration of products Pyr1 and Pyr2. This is due to the fact that the products form a protective film absorbed by the steel, the layer of the film increases with increasing the inhibitor concentration, which protects the surface of the mild steel efficiently. In absence of the inhibitor the corrosion rate is $0.3514 \text{ mg/cm}^2 \text{ h}$, by cons at a concentration of 10^{-3} of products Pyr1 and Pyr2 the corrosion rate it reaches $0.0305 \text{ mg/cm}^2 \text{ h}$ and $0.0512 \text{ mg/cm}^2 \text{ h}$ respectively. The resultats show also that for all concentrations η_{WL} (Pyr1) is greater than η_{WL} (Pyr2), so we can say that the product Pyr1 is more effective than the product Pyr2.

3.2. Effect of Temperature

The study of the effect of temperature is performed using the mild steel weight loss of data in a solution of 1M HCl to temperatures ranging from 303 K to 333 K in the absence and the presence of 10^{-3}M of inhibitors Pyr1 and Pyr2 for 1h of immersion time. The results are presented in Table 2.

Table 1: Effect of concentration of Pyr1 and Pyr2 on the corrosion rate of mild steel in 1M HCl at 308 K

Medium	Conc (M)	C_R (mg/cm ² h)	η_{WL} (%)	θ
Blank	1	0.3514	--	--
Pyr1	10 ⁻⁶	0.2445	30	0.30
	10 ⁻⁵	0.1775	49	0.49
	5.10 ⁻⁵	0.1356	61	0.61
	10 ⁻⁴	0.0756	78	0.78
	5.10 ⁻⁴	0.0516	85	0.85
	10 ⁻³	0.0305	91	0.91
Pyr2	10 ⁻⁶	0.2698	23	0.23
	10 ⁻⁵	0.1914	45	0.45
	5.10 ⁻⁵	0.1526	56	0.56
	10 ⁻⁴	0.1043	70	0.70
	5.10 ⁻⁴	0.0698	80	0.80
	10 ⁻³	0.0512	85	0.85

Table 2: Effect of temperature on the corrosion of mild steel in 1 M HCl of product Pyr1 and Pyr2 at 10⁻³M for 1h

Medium	Temp (K)	C_R (mg cm ⁻² h ⁻¹)	η_{WL} (%)
Blank	303	0.198	--
	313	0.542	--
	323	1.471	--
	333	2.719	--
Pyr1	303	0.0384	80.6
	313	0.1220	77.4
	323	0.5697	61.2
	333	1.2936	52.4
Pyr2	303	0.0545	72.4
	313	0.2172	59.9
	323	0.8258	43.8
	333	1.8521	31.8

Inspection of Table 2 showed that corrosion rate increased with increasing temperature in uninhibited and inhibited solutions while the inhibition efficiency of Pyr1 and Pyr2 decreased with increasing temperature.

The results show that inhibition efficiency decreases with temperature increasing. The activation parameters for the corrosion process were calculated from Arrhenius type plot according to the following [33]:

$$C_R = A \exp\left(-\frac{E_a}{RT}\right) \quad (4)$$

Where A is the Arrhenius preexponential constant, E_a is the apparent activation corrosion energy, R is the universal gas constant and T is the absolute temperature.

And the alternative formulation of Arrhenius equation is:

$$C_R = \frac{RT}{Nh} \exp\left(\frac{\Delta S_a}{R}\right) \exp\left(-\frac{\Delta H_a}{RT}\right) \quad (5)$$

Where ΔS_a is the entropy of activation, ΔH_a is the enthalpy of activation, N is Avagadro's number and h is Planck's constant. Arrhenius plots for the corrosion rate of steel are given in (Figure 1). Values of (E_a) for steel in 1 M HCl without and with 10⁻³ of Pyr1 and Pyr2 product were calculated by linear regression between Ln (C_R) and 1/T. The results are shown in Table 3. The value of E_a determined in 1M HCl containing inhibitors is higher (100.18 kJ mol⁻¹ and 101.55 kJ mol⁻¹) than that for uninhibited solution (74.468 kJ mol⁻¹). The increase in

the apparent activation energy may be interpreted as physical adsorption that occurs in the first stage [34]. The increase in activation energy can be attributed to decrease in the adsorption of the inhibitor on the steel surface with increase in temperature.

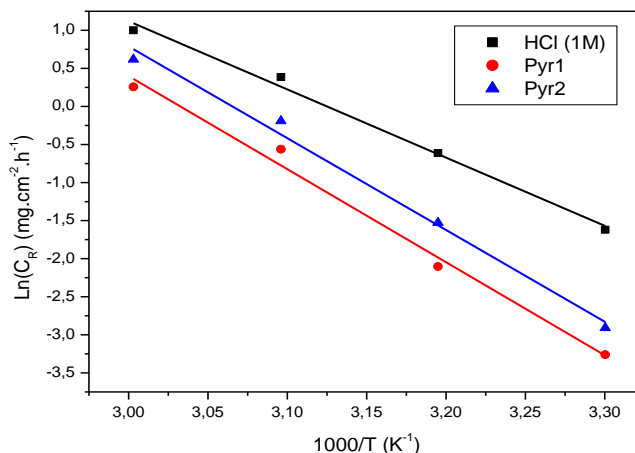


Figure 1: Arrhenius Plots in the absence and presence of product Pyr1 and Pyr2 in 1M HCl

As adsorption decreases more desorption of inhibitor molecules occurs because these two opposite processes are in equilibrium. owing to the desorption of inhibitor molecules at higher temperatures the greater surface area of steel comes in contact with aggressive environment, resulting increased corrosion rates with increase in temperature [35,36]. Figure 2 shows the variation of $\text{Ln}(C_R/T)$ function ($1/T$) as a straight line with a slope of $(-\Delta H_a/R)$ and the intersection with the y-axis is $[\text{Ln}(R/Nh) + (\Delta S_a/R)]$. From these relationships, values of ΔS_a and ΔH_a can be calculated. The activation parameters (E_a , ΔH_a and ΔS_a) calculated from the slopes of Arrhenius lines in the absence and presence of our inhibitors (Fig.1 and Fig.2) are summarized in Table 3.

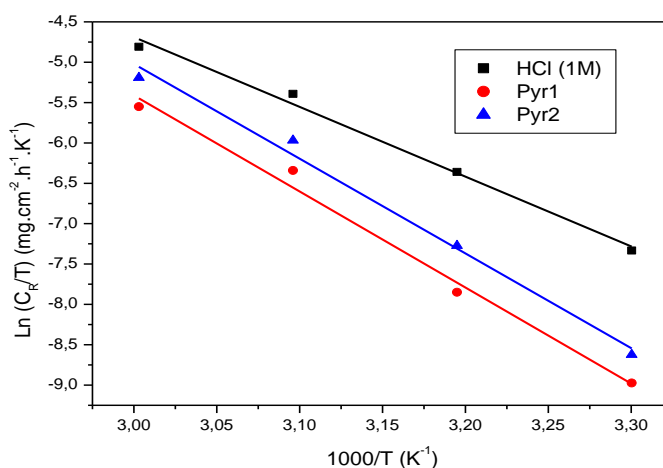


Figure 2: Variation of $\text{Ln}(C_R/T)$ versus $1000/T$ for 10^{-3} of Pyr1 and Pyr2 in 1M HCl

Table 3: Activation parameters for the steel dissolution in HCl with and without 10^{-3} M of inhibitors

Medium	Conc (M)	E_a (kJ mol ⁻¹)	ΔH_a (kJ mol ⁻¹)	ΔS_a (J mol ⁻¹ K ⁻¹)	$E_a - \Delta H_a$
Blank	1 M	74.47	71.83	-20.97	2.64
Pyr1	10^{-3}	100.18	97.54	53.41	2.64
Pyr2	10^{-3}	101.55	98.92	54.29	2.64

Inspection of these data reveals that the ΔH_a values for dissolution reaction of steel in 1M HCl in the presence of inhibitors are higher (97.54 and 98.92 kJ mol⁻¹) than that of the absence of inhibitors (71.83 kJ mol⁻¹). The positive signs of ΔH_a reflect the endothermic nature of the steel dissolution process suggesting that the dissolution of steel is slow in the presence of inhibitors [37-41]. Also, for all systems, the average value of the difference between E_a and ΔH_a is about (2.64 kJ mol⁻¹) which approximately around the average value of RT (2.68 kJ mol⁻¹).

$$E_a - \Delta H_a = RT \quad (6)$$

3.2.1. Adsorption isotherm and thermodynamic parameters

Adsorption isotherms are usually used to describe the adsorption process. The most frequently used isotherms include: Langmuir, Frumkin, Temkin Flory–Huggins, Dhar–Flory–Huggins, Bockris–Swinkels. Adsorption of the organic molecules occurs as the interaction energy between molecule and metal surface is higher than that between the H₂O molecule and the metal surface. The simple mechanistic picture of the adsorption process was proposed by Langmuir. Langmuir isotherm assumes that:

- The metal surface contains a fixed number of adsorption sites and each site holds one adsorbate;
- ΔG_{ads}° is the same for all sites and it is independent of the surface coverage, $\theta = E \% / 100$;
- The adsorbates do not interact with one another, i.e., there is no effect of lateral interaction of the adsorbates on ΔG_{ads}° [42,43].

The Langmuir adsorption isotherm given a relatively simple mathematical expression of C , the concentration of inhibitor K , the adsorptive equilibrium constant and θ , may be written in the following rearranged form:

$$\frac{C}{\theta} = \frac{1}{K} + C \quad (7)$$

The adsorption isotherm parameters and correlation coefficients found from the slopes and intercepts are summarized in Table 4 from Figure 3. The Langmuir adsorption isotherm is the best fit was made according to the correlation coefficient since $R^2 > 0.99$ [44,45]. Langmuir adsorption isotherm assumes that the adsorption of organic molecules on the adsorbent is monolayer.

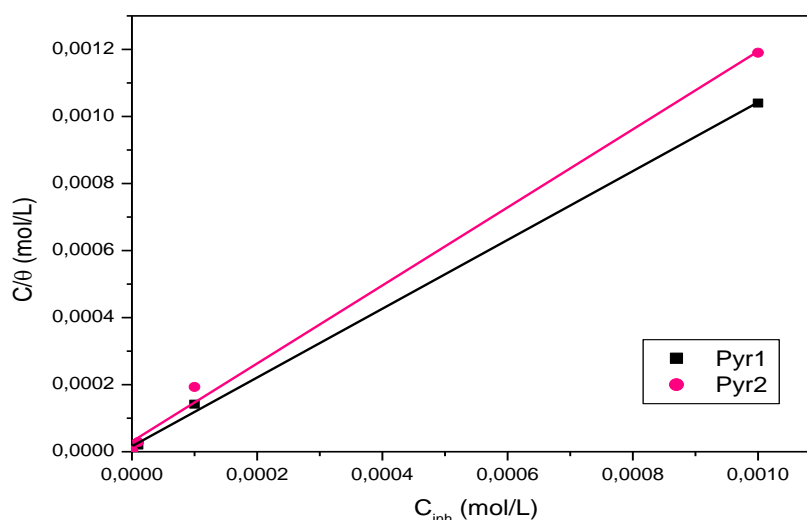


Figure 3: Langmuir adsorption of Pyr1 and Pyr2 on the mild steel in 1M HCl

Table 4: Parameters of the linear regression between C/θ and C and thermodynamic values of adsorption product on the steel mild in 1M HCl.

Inhibitors	Linear correlation	Slope
Pyr1	0.9989	1.03
Pyr2	0.9967	1.16

The well-known thermodynamic adsorption parameters are the free energy of adsorption ($\Delta G^{\circ}_{\text{ads}}$), the standard enthalpy of adsorption ($\Delta H^{\circ}_{\text{ads}}$) and the entropy of adsorption ($\Delta S^{\circ}_{\text{ads}}$). These quantities can be calculated depending on the estimated values of K_{ads} from adsorption isotherms, at different temperatures. The constant of adsorption, K_{ads} , is related to the standard free energy of adsorption $\Delta G^{\circ}_{\text{ads}}$, with the following equation [46]:

$$K_{\text{ads}} = \frac{1}{C_{\text{H}_2\text{O}}} \exp\left(\frac{-\Delta G^{\circ}_{\text{ads}}}{RT}\right) \quad (8)$$

Where R is the universal gas constant, T the thermodynamic temperature and the concentration of water in the solution is 55.5 mol/L. The calculated $\Delta G^{\circ}_{\text{ads}}$ values, at all studied temperatures, are given in Table 5.

Table 5: Adsorption parameters of the linear regression between C/θ and C of Pyr1 and Pyr2

T (K)	K_{ads} (10^4 M^{-1})	$\Delta G^{\circ}_{\text{ads}}$ (KJ mol $^{-1}$)
Pyr1	10.257	-39.17
Pyr2	14.294	-40.02

Generally, the adsorption type is regarded as physisorption if the absolute value of $\Delta G^{\circ}_{\text{ads}}$ is in the range of 20 kJ.mol $^{-1}$ or lower. The inhibition behaviour is attributed to the electrostatic interaction between the organic molecules and steel surface. When the absolute value of $\Delta G^{\circ}_{\text{ads}}$ is in the order of 40 KJ mol $^{-1}$ or higher, the adsorption could be seen as chemisorption. In this process, the covalent bond is formed by the charge sharing or transferring from the inhibitor molecules to the metal surface [47-49]. The obtained $\Delta G^{\circ}_{\text{ads}}$ values in the studied temperature domain are in the range of -39.15 to -40.01 kJ mol $^{-1}$, indicating, therefore that the adsorption mechanism of Pyr1 and Pyr2 onto mild steel in 1 M HCl solution is mainly due to Chemisorption (Table 5).

3.2. Polarization curves

The polarization curves of mild steel in 1M HCl obtained with and without various concentrations of Pyr1 and Pyr2 products are shown in (Fig.4, Fig.5). Electrochemical parameters such as Tafel slope constants calculated from Tafel plots (β_c), corrosion current density (I_{corr}), and the inhibition efficiency ($E_1\%$) and corrosion potential (E_{corr}) were determined by Tafel extrapolation method and given in Table 6.

The values of inhibition efficiency ($E_1\%$) were calculated using the following equation:

$$E_1\% = \frac{I_{\text{corr}} - I_{\text{corr}}(\text{inh})}{I_{\text{corr}}} \times 100 \quad (9)$$

Where I_{corr} and $I_{\text{corr}}(\text{inh})$ are the values of corrosion current densities of steel without and with the additive, respectively, which were determined by extrapolation of the cathodic Tafel lines to the corrosion potential E_{corr} .

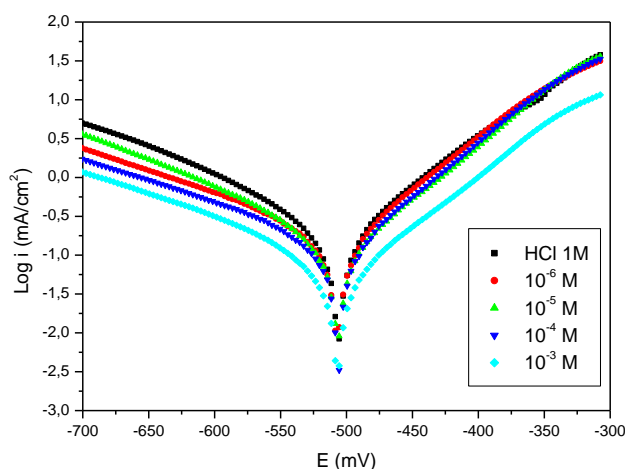


Figure 4: Polarization curves of steel in 1M HCl containing various concentrations of Pyr1

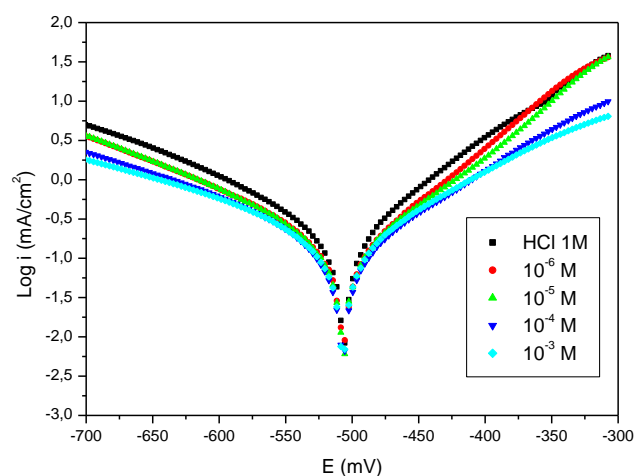


Figure 5: Polarization curves of steel in 1M HCl containing various concentrations of Pyr2

From table 5 and (Fig.4, Fig.5), it is seen that the addition of various concentrations of inhibitors Pyr1 and Pyr2 affects the polarization curves and therefore reduces I_{corr} significantly, due to the increase of the blocked fraction of the adsorption electrode surface. These results demonstrated that the hydrogen evolution reaction is inhibited and the inhibition efficiency increases with increasing concentration of inhibitors. Inhibition efficiency (E_i) 10^{-3} M reached 84.9% for Pyr1 and 78.6% for Pyr2, which once again confirms that both inhibitors are a good steel inhibitors in 1 M HCl, and E_i following order: Pyr1> Pyr2 [50]. If the shift in the corrosion potential is greater than ± 85 mV / SCE with respect to the potential of the blank corrosion inhibitor can be considered as an anodic or cathodic, but the maximum displacement in this case is less than 20 mV / SCE, indicating that the two products Pyr1 and Pyr2 are mixed type inhibitors [51]. If the change in E_{corr} is negligible, the inhibition is very probably caused by a geometric blocking effect inhibitory species adsorbed on the surface to corrode the metal [52].

Table 6: Polarization data of mild steel in 1M HCl without and with addition of inhibitors

Medium	Conc (M)	E_{corr} (mV/SCE)	I_{corr} (mA/cm ²)	β_c (mV/dec)	E_i (%)
Blank	1 M	-506.5	0.3818	-172.4	--
Pyr1	10^{-6}	-503.2	0.2509	-150.9	34.2
	10^{-5}	-506.3	0.1630	-184.7	57.3
	10^{-4}	-512.0	0.1248	-151.1	67.3
	10^{-3}	-509.1	0.0575	-148.4	84.9
Pyr2	10^{-6}	-517.3	0.2714	-175.2	28.9
	10^{-5}	-508.4	0.2319	-216.5	39.2
	10^{-4}	-514.2	0.1382	-151.7	63.8
	10^{-3}	-507.8	0.0816	-155.9	78.6

3.3. Electrochemical Impedance Spectroscopy (EIS)

The corrosion behavior of mild steel, in acidic solution containing different concentration of Pyr1 compound, was investigated on a newly polished steel surface by the EIS at 308 K after 30 min of immersion. The obtained results are presented in Fig. 6. Impedance parameters derived from the Nyquist plots are given in Table 7. The charge transfer resistance, R_{ct} values are calculated from the difference in impedance at lower and higher frequencies [53]. To obtain the double layer capacitance (C_{dl}), the frequency at which the imaginary component of the impedance is maximum ($-Z_{max}$) is found and C_{dl} values are obtained from the equation:

$$f(-Z_{max}) = \frac{1}{2\pi C_{dl} R_{ct}} \quad (10)$$

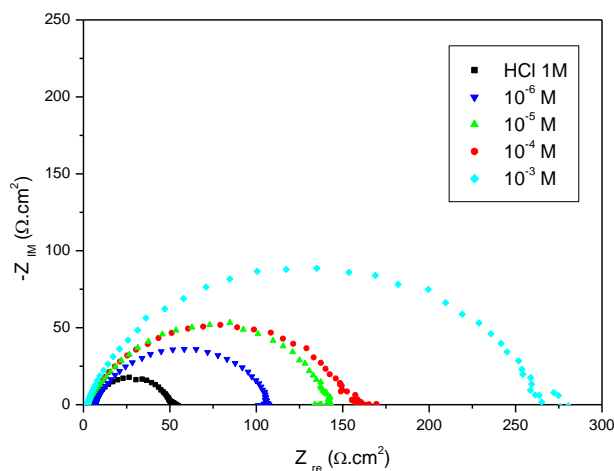


Figure 6: Nyquist diagrams for mild steel in 1M HCl containing different concentrations of Pyr1.

Figure 6 represent the Nyquist diagrams for mild steel in 1 M HCl in the presence of Pyr1 product. The impedance spectra present a large capacitive loop at high frequencies followed by a small inductive loop at low frequency values. In the presence of Pyr1 product, comparing with blank solution, the shape is maintained throughout all tested concentrations, indicating that almost no change in the corrosion mechanism occurs due to the inhibitor addition [54]. The capacitive loop indicates that the corrosion of steel is mainly controlled by a charge transfer process, and usually related to the charge transfer of the corrosion process and double layer behavior. The inhibition efficiency is calculated using charge transfer resistance from the equation [55]:

$$\eta\% = \frac{R_{ct(inh)} - R_{ct}}{R_{ct(inh)}} \times 100 \quad (11)$$

Where R_{ct} and $R_{ct(inh)}$ are the charge transfer resistance values in absence and presence of inhibition for steel in 1M HCl, respectively

Table 7: Characteristic parameters evaluated from the impedance diagram of Pyr1 in 1M HCl

Medium	Conc (M)	R_{ct} ($\Omega \text{ cm}^2$)	C_{dl} ($\mu\text{F}/\text{cm}^2$)	η (%)
Blank	1 M	52.3	66.30	--
Pyr1	10^{-6}	101.6	187.1	48.5
	10^{-5}	142.7	159.1	63.3
	10^{-4}	162.8	102.6	67.8
	10^{-3}	243.5	85.7	78.5

By increasing the inhibitor concentration the R_t values increase but C_{dl} values decrease. According to Helmholtz model, the double layer capacitance C_{dl} is given by:

$$C_{dl} = \frac{\epsilon_0 \epsilon}{\delta} S \quad (12)$$

Where ϵ is the medium dielectric constant, ϵ_0 is the permittivity of the air, δ is the thickness of the deposit and S is the surface of the electrode.

Fig. 7 represent the evolution of the double layer capacitance with the inhibition efficiency of Pyr1, this decrease in C_{dl} values with the addition of inhibitor is due to the adsorption of the inhibitor molecules replacing water at the metal–solution interface that led to the decrease in local dielectric constant and/or an increase in the thickness of the electrical double layer [56-58].

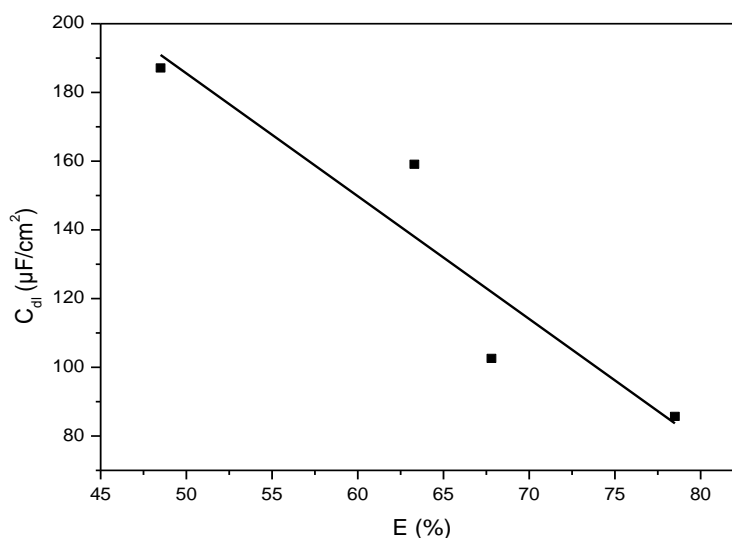


Figure 7: Evolution of C_{dl} with the inhibition efficiency of Pyr1.

3.4. Scanning electron microscopy

The scanning electron microscope (SEM) images has become an essential tool to study the surface morphology of corroded and uncorroded metals, in order to analyse the interaction between the inhibitors and the steel surface, SEM images were recorded for mild steel coupons in the absence and presence of Pyr1 and Pyr2 at the optimal concentration the results are shown in Figure 8.

The electron micrographs reveal a smooth surface in absence of any treatment Fig. 8a, however, after an immersion in HCl medium for 6 hour, the surface was strongly damaged owing to corrosion in absence of the inhibitor Fig. 8b, but in the presence of the inhibitor there is a much smaller damage on the surface Fig. 8c and Fig. 8d. This is attributed to the formation of a good protective film on the mild steel surface. On comparison Pyr1 acts as good inhibitor than pyr2 at the same concentration.

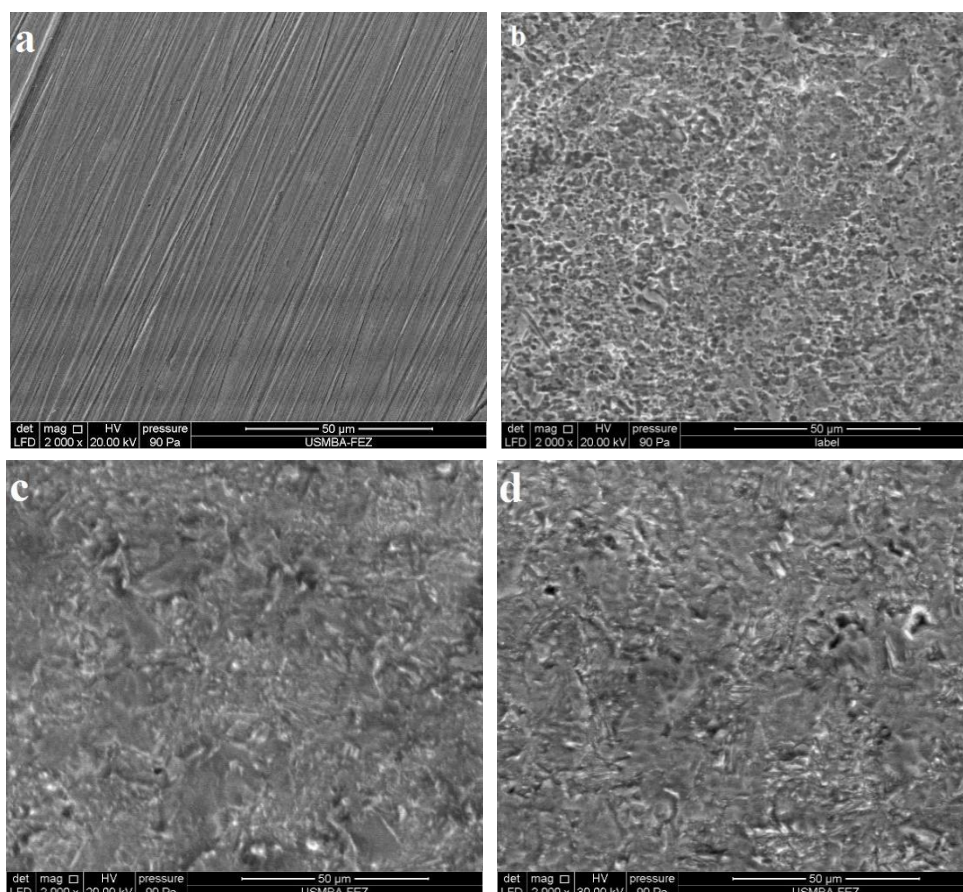


Figure 8: SEM of mild steel: (a) steel polished; (b) steel immersed at 6 h in 1 M HCl; (c) Steel immersed at 6 h in 1 M HCl + 10^{-3} M of Pyr1 (d) Steel immersed at 6 h in 1 M HCl + 10^{-3} M of Pyr2

Conclusion

1. Both products Pyr1 and Pyr2 are considered as good inhibitors for mild steel corrosion in 1M HCl.
2. The inhibition efficiency increases with increasing inhibitor concentrations to attain a maximum value of 91 % for Pyr1 and 85% for Pyr2 at 10^{-3} M.
3. The inhibition efficiency decreased with increasing temperature.
4. Polarization study shows that Pyr1 and Pyr2 act as a mixed-type inhibitor.
5. Pyr1 and Pyr2 adsorbs on the steel surface according to the Langmuir isotherm. Moreover, the calculated values of ΔG°_{ads} reveal that the adsorption mechanism of Pyr1 and Pyr2 on steel surface in 1 M HCl solution is mainly chemisorption
6. SEM investigations show that the addition of Pyr1 and Pyr2 in 1M HCl in solution forms a film on the steel surface, which causes the decrease of the roughness of the metal surface and strongly protects the surface of the steel against corrosion.

References

1. Batros M., Hakerman N., *Electrochem J., Soc.* 139 (1992) 3429.
2. Bentiss F., Lagrenee M., Traisnel M., Mernari B., El Attari H., *J. Appl. Electrochem.* 29 (1999) 1073.
3. Kutej P., Vosta J., Pancir J., Macak J., Hackerman N., *J. Electrochem. Soc.* 142 (1995) 829.
4. Dahmani M., Et-Touhami A., Al-Deyab S.S., Hammouti B., Bouyanzer A., *Int J. Electrochem. Sci.* 5 (2010) 1060.
5. Bastidas J.M., Polo J.L., Cano E., *J. Electrochem. Soc.* 30 (2000) 1173.
6. Hammouti B., Zarrouk A., Al-Deyab S.S., Warad I., *Orient. J. Chem.*, 27 (2011) 23
7. Fouda A., Mahfouz H., *Chil J., Chem. Soc.*, 54 (2009) 408
8. Elouali I., Hammouti B., Aouniti A., Ramli Y., Azougagh M., Essassi E.M., Bouachrine M., *J. Mater. Environ. Sci.*, 1 (2009) 1
9. Ghibate R., Sabry F., Kharbach Y., KandriRodi Y., Skalli M.K., Haoudi A., Senhaji O., Touzani M., Taouil R., Aouniti A., Hammouti B., *Int. J. Eng. Res. App.* 5 (12) (2015) 22-30.
10. Ghazoui A., Zarrouk A., Bencat N., Salghi R., Assouag M., El Hezzat M., Guenbour A., Hammouti B., *J. Chem. Pharm. Res.* 6 (2014) 704.
11. Zarrok H., Zarrouk A., Salghi R., Ramli Y., Hammouti B., Al-Deyab S.S., Essassi E.M., Oudda H., *Int. J. Electrochem. Sci.* 7(9) (2012) 8958.
12. Bendaha H., Zarrouk A., Aouniti A., Hammouti B., El Kadiri S., Salghi R., Touzan R., *Phys. Chem. News* 64 (2012) 95.
13. Zarrouk A., Hammouti B., Zarrok H., Salghi R., Dafali A., Bazzi L., Bammou L., Al-Deyab S.S., *Der Pharm. Chem.* 4(1) (2012) 337.
14. Ghazoui A., Saddik R., Benchat N., Hammouti B., Guenbour M., Zarrouk A., Ramdani M., *Der Pharm. Chem.* 4(1) (2012) 352.
15. Zarrouk A., Hammouti B., Zarrok H., Bouachrine M., Khaled K.F., Al-Deyab S.S., *Int. J. Electrochem. Sci.* 6 (2012) 89.
16. Zarrok H., Zarrouk A., Salghi R., Assouag M., Hammouti B., Oudda H., Boukhris S., Al Deyab S.S., Warad I., *Der Pharm. Lett.* 5 (2013) 43.
17. Zarrok H., Saddik R., Oudda H., Hammouti B., El Midaoui A., Zarrouk A., Benchat N., EbnTouhami M., *Der Pharm. Chem.* 3(5) 2011) 272.
18. Zarrouk A., Hammouti B., Touzani R., Al-Deyab S.S., Zertoubi M., Dafali A., Elkadiri S., *Int. J. Electrochem. Sci.* 6 (10) (2011) 4939.
19. Kertit S., Hammouti B., *Appl. Surf. Sci.*, 93 (1996) 59
20. Chetouani A., Hammouti B., Aouniti A., Benchat N., Benhadda T., *Prog. Org. Coat.*, 45(2002) 373
21. Bekkouch K., Aouniti A., Hammouti B., Kertit S., *J. Chim. Phys.*, 96(1999) 838
22. Kertit S., Hammouti B., Taleb M., Brighli M., *Bull. Electrochem.* 13(1997) 241
23. Bouklah M., Benchat N., Aouniti A., Hammouti B., Benkaddour M., Lagrenee M., Vezin H., Bentiss F., *Prog. Org. Coat.*, 51 (2004) 118
24. Wang L., *Corros. Sci.*, 48 (2006) 608
25. Lagrenee M., Mernari B., Chaibi N., Traisnel M., Vezin H., Bentiss F., *Corros. Sci.*, 43 (2001) 951
26. Rengamani S., Muralidharan S., AnbuKulandainathan M., VenkatakrishnaIyer S., *J. Electrochem. Soc.*, 24 (1994) 355
27. Bentiss F., Gassama F., Barbry D., Gengembre L., Vezin H., Lagrenée M., Traisnel M., *Appl. Surf.Sci.* 252 (2006) 2684.
28. Chetouani A., Hammouti B., Aouniti A., Benchat N., Benhadda T., *Prog. Org. Coat.* 45 (2003) 73.
29. Chetouani A., Aouniti A., Hammouti B., Benchat N., Benhadda T., Kertit S., *Corros. Sci.* 45 (2003) 1675.
30. Negm N.A., Al Sabagh A.M., Migahed M.A., Abdel Bary H.M., El Din H.M., *Corros. Sci.*, 52 (2010) 2122.
31. Qi Zhang, Zhinong Gao, Feng Xu, Xia Zou, *Colloids and Surfaces A: Physicochemical andEngineering Aspects.*, 380(2011) 191.

32. Bourichi S., Kandri Rodi Y., Misbahi K., Ouazzani Chahdi F., Akhazzane M., Essassi E.M., *J.mar.chim.heterocycl.* 14 (2015) 70-71
33. Lebrini M., Robert F., Roos C., *Int. J. Electrochem. Sci.*, 6 (2011) 847.
34. Guan N.M., Xueming L., Fei L., *Mater. Chem. Phys.* 86 (2004) 59.
35. Tsuru T., Haruyama S., Gijutsu B., *J. Jpn. Soc. Corros. Eng.* 27 (1978) 573.
36. Haloui T., Kharbach Y., Tribak Z., El Azzouzi M., Aouniti A., Hammouti B., B Alaoui A., *Der. Pharma. Chemica.* 7 (9) (2015) 225-238
37. Guan N. M., Xueming L., Fei L., *Mater. Chem. Phys.* 86 (2004) 59.
38. Kharbach Y., Haoudi A., Skalli M.K., Kandri Rodi Y., Aouniti A., Hammouti B., Senhaji O., Zarrouk A., *J. Mater. Environ. Sci.* 6 (10) (2015) 2906-2916.
39. Bendaif H., Melhaoui A., El Azzouzi M., Legssyer B., Hamat T., Elyoussfi A., Aouniti A., El Ouadi Y., Aziz M., *J. Mater. Environ. Sci.* 7 (4) 1276-1287
40. Yousfi F., El Azzouzi M., Ramdani M., Elmsellem H., Aouniti A., Saidi N., El Mahi B., Chetouani A., Hammouti B., *Der Pharma Chemica* 7 (7) (2016) 377-388
41. El Azzouzi M., Aouniti A., Herrag L., Chetouani A., Elmsellem H., Hammouti B., *Der Pharma Chemica* 7(2)201512-24.
42. Chetouani A., Hammouti B., Aouniti A., Benchat N., Benhadda T., *Prog. Org. Coat.*, 45 (2002) 373.
43. El-Hajjaji F., Taleb M., Rais Z., Saddik R., Elaataoui A., Hammouti B., *J. Alloys Compounds*, 693 (2017) 510-517
44. Flis J., Zakroczymski T., *J. Electrochem. Soc.*, 143 (1996) 2458.
45. Popova A., Christov M., Zwetanova A., *Corros. Sci.*, 49 (2007) 2131.
46. El Azhar M., Traisnel, M., Mernari, B., Gengembre, L., Bentiss, F., Lagrenée, M., *App. Surf. Sci.* 185 (2010) 197.
47. Donahue F. M., Nobe, K., *J. Electrochem. Soc.* 112 (1965) 886.
48. Khamis E., Bellucci, F., Latanision, R. M., El-Ashry, E. S. H. *Corrosion.* 47 (1991) 677.
49. Tourabi M., Nohair K., Nyassi A., Hammouti B., Jama C., Bentiss F., *J. Mater. Environ. Sci.* 5 (2014) 1133-1143
50. Ferreira E.S., Giancomelli C., Giancomelli F.C., Spinelli A., *Mater. Chem. Phys.*, 83 (1) (2004) 129-134.
51. O.L. Riggs Jr, in *Corrosion Inhibitors*, ed. by C.C. Nathan (The National Association of Corrosion Engineers (NACE), Houston, (1973), pp. 2–27
52. Cao C., *Corros. Sci.*, 38 (1996) 2073.
53. Tsuru T., Haruyama S., Gijutsu B., *J. Jpn. Soc. Corros. Eng.*, 27 (1978) 573
54. Labjar N., Lebrini M., Bentiss F., Chihib N.E., El Hajjaji S., Jama C., *Mater. Chem. Phys.* 6 (2010) 119.
55. Gopi D., Govindaraju K. M., Kavitha L., *J. Appl. Electrochem.* 40 (2010) 1349.
56. Souli R., Triki E., Berçot P., Rezrazi M., Jaouad B., Derja A., Dhouibi L., *J. Mater. Environ. Sci.* 6 (2015) 2729-2731.
57. Fouda A. S., Abdallah Y. M., Elawady G. Y., Ahmed R. M., *J. Mater. Environ. Sci.* 6 (2015) 1519- 1531.
58. Tribak Z., Kharbach Y., Haoudi A., Skalli M.K., Kandri Rodi Y., El Azzouzi M., Aouniti A., Hammouti B., Senhaji O., *J. Mater. Environ. Sci.* 7 (6) (2016) 2006-2020

(2017) ; <http://www.jmaterenvironsci.com>